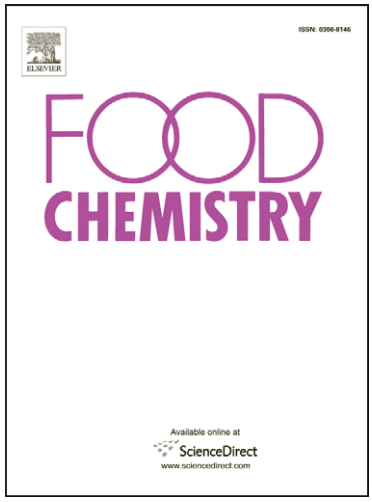

Nutrition analysis by nano-particle assisted laser desorption/ionization mass spectrometry

Yuko Sahashi, Issey Osaka, Shu Taira

PII: S0308-8146(10)00568-6
DOI: 10.1016/j.foodchem.2010.05.008
Reference: FOCH 9615

To appear in: *Food Chemistry*

Received Date: 19 November 2009
Revised Date: 25 March 2010
Accepted Date: 1 May 2010

Please cite this article as: Sahashi, Y., Osaka, I., Taira, S., Nutrition analysis by nano-particle assisted laser desorption/ionization mass spectrometry, *Food Chemistry* (2010), doi: 10.1016/j.foodchem.2010.05.008

Nutrition analysis by nano-particle assisted laser desorption/ionization mass spectrometry.

Yuko Sahashi[1], Issey Osaka[2] and Shu Taira[3*]

[1] *Nitto Denko Corporation 1-1-2 Shimohozumi, Ibaraki, Osaka 567-8680, Japan*

[2] *Japan Advanced Institute of Science and Technology, Center for Nano Materials and Technology, 1-1 Asahidai, Nomi, Ishikawa 923-1292, Japan*

[3] *Japan Advanced Institute of Science and Technology*
School of Material Science 1-1 Asahidai, Nomi city, Ishikawa 923-1292, Japan

[*]Corresponding author. e-mail: s-taira@jaist.ac.jp

Abstract

We analyzed the bioactive compounds in *Panax ginseng* C.A. Meyer by using nanoparticle-assisted laser desorption/ionization (nano-PALDI) mass spectrometry (MS). To this end, we prepared manganese oxide nanoparticles (d = 5.4 nm) and developed a nano-PALDI MS method to analyze the standard ginsenosides and identify these ginsenosides in an extract of *Panax ginseng*. The nanoparticles served as an ionization-assisting reagent in MS. The mass spectra did not show any background interference in the low-m/z range. Our pilot study showed that the nanoparticles could ionize the standard ginsenosides and also respective lipid and ginsenosides in the extract without the aid of chemical and liquid matrices used in conventional MS methods. Analysis of the post-source decay spectra obtained using nano-PALDI MS will yield information regarding the chemical structure of the analyte.

Introduction

Herbal products have been used in traditional Chinese medicine (TCM) for a long time and have recently gained attention as complementary and alternative medicines (Hijikata, Miyamae, Takatsu & Sentoh, 2007; Sun et al., 2009; Xu & Xu, 2009). *Panax ginseng* C.A. Meyer is one of the most famous oriental herbs used in TCM, and it contains many bioactive compounds, including triterpene glycosides called ginsenosides. Although ginsenosides have been thought to be the main bioactive components in *Panax ginseng* (Metori, Furutsu & Takahashi, 1997; Newman et al., 1992; Wu et al., 1992), their role in the efficacy of *Panax ginseng* has not been completely elucidated. Recent articles have reported that multiple components in *Panax ginseng*, such as lipids, polysaccharides, peptides, and amino acids act synergistically (Spelman, Burns, Nichols, Winters, Ottersberg & Tenborg, 2006; Zeng, Liang, Jiang, Chau & Wang, 2008). Therefore, to elucidate the efficacy of this herb, simultaneous analysis of the secondary-metabolite complexes of relatively small molecules like ginsenosides is very important.

Mass spectrometry (MS) is a powerful technique used to analyze metabolites in biological samples and tissues. It can be used to directly and simultaneously detect multiple components in crude samples such as TCM products. Although MS combined

with liquid chromatography (LC) and gas chromatography (GC) can be used to analyze ginsenosides (Cui, Song, Liu & Liu, 2001; Fuzzati, Gabetta, Jayakar, Pace & Peterlongo, 1999; Li, Mazza, Cottrell & Gao, 1996; Tawab, Bahr, Karas, Wurglics & Schubert-Zsilavecz, 2003; Wang et al., 2008), these techniques are time consuming (analysis time, ~30 min.). Matrix-assisted laser desorption/ionization (MALDI) MS is a soft and sensitive ionization technique that uses chemical matrices such as 4-hydroxy-α-cinnamic acid (CHCA), 2,5-dihydroxybenzoic acid (DHB), and sinapic acid (SA) to facilitate ionization of the analyte. However, one of the main problems of MALDI-MS is the overlapping of the matrix peaks and fragment peaks in the low-mass region (*m/z* ~ 800). These shortcomings significantly complicate the application of these techniques in the multiple-component analysis of samples such as TCM products and their metabolites. It is our approach that these shortcomings can be overcome by using advanced analytical techniques developed through interdisciplinary collaboration.

Nanomaterials have shown great potential in facilitating the development of new technologies (Chithrani & Chan, 2007; Moritake et al., 2007; Taira, Hatanaka, Moritake, Kai, Ichiyanagi & Setou, 2007). Nanoparticles (NPs) have been used in the development of solar cells (Kitada, Kikuchi, Ohono, Aramaki & Maenosono, 2009), sensors (Ai, Zhang & Lu, 2009; Kalogianni, Koraki, Christopoulos & Ioannou, 2006),

64 catalysts (Mitsudome, Noujima, Mizugaki, Jitsukawa & Kaneda, 2009), drug delivery
65 systems (Moritake et al., 2007), and imaging techniques (Taira, Sugiura, Moritake,
66 Shimma, Ichiyanagi & Setou, 2008). However, there have been very few studies on the
67 use of NPs in food chemistry (Ravindranath, Mauer, Deb-Roy & Irudayaraj, 2009; Yang,
68 Kostov, Bruck & Rasooly, 2009). Previous studies used photospectroscopy with NPs to
69 detect analytes; however, this technique afforded limited detection of the multiple
70 components in food. In our previous reports, to obtain ionization-assisting agents that
71 could be used to perform nanoparticle-assisted laser desorption/ionization
72 (nano-PALDI) MS without significantly increasing the background signals, we prepared
73 metal oxide nanoparticles surrounded by amorphous SiO_2 and an amino group (Figure 1
74 c and d) (Moritake, Taira, Sugiura, Setou & Ichiyanagi, 2009; Taira, Kitajima,
75 Katayanahi, Ichiishi & Ichiyanagi, 2009; Taira et al., 2008). Here, we investigated the
76 suitability of nano-PALDI MS for analyzing lipid and ginsenosides in *Panax ginseng*
77 extracts. We assessed the ionization of several standard ginsenosides by using
78 nano-PALDI MS as an analysis marker for crude samples. Further, we used the
79 nano-PALDI MS technique to separate and evaluate the original ingredients in the
80 complicated MS spectrum for ginseng extract.

81 **Method**

Materials

Standard ginsenosides (Rb_1, Rb_2, Rc, Rd, Re, Rf, and Rg_1 with purity >98 %, >94%, >99%, >99%, >99%, >99%, and >99%, respectively) were purchased from Funakoshi (Tokyo, Japan). The extract was obtained from tissue-cultured *Panax ginseng* (TCPG) (Nitto Denko, Osaka, Japan). The TCPG powder was extracted using hot water (80°C) for 2 h, dried, and re-extracted with 70% (v/v) methanol. The extract thus obtained was applied to a small column (Sep-Pak cartridge C18 and NH_2; Waters, Milford, USA) to concentrate the ginsenosides.

Preparation of nanoparticles

Manganese oxide-based nanoparticles were prepared by mixing aqueous solutions of $MnCl_2 \cdot 4H_2O$ (5 ml, 100 mM; WAKO Pure Chemicals, Japan) and 3-aminopropyltriethoxysilane (5 ml; γ-APTES; Shinetsu, Kagaku, Japan). After stirring at room temperature for 1 h, the resulting precipitate was washed several times with ultrapure water and dried at 55°C in an incubator. The dried samples were pulverized in a porcelain mortar. The morphology and diameter distribution of the nanoparticles were investigated using a transmission electron microscope (TEM; H-7100; Hitachi, Japan).

Nano-PALDI mass spectrometry

The utility of the nanoparticles as ionization-assisting materials in mass spectrometry was confirmed in a MALDI-TOF-type instrument (TOF = time of flight; Voyager-DE-RP; Applied Biosystems, Germany) by using a N_2 laser with an emission wavelength of 337 nm. Samples of standard ginsenosides samples such as G-Rb_1, G-Rb_2, G-Rc, G-Rd, G-Re, G-Rf, and G-Rg_1 were chosen for the analysis. The nanoparticles (1 mg) were dispersed in 1 mL of methanol or in 1 mL of a 10 mM methanolic solution of sodium acetate. Each sample was independently dissolved in distilled water at a concentration of 100 pmol/μL. Each analyte solution (1 μL) was pipetted on to the surface of the nanoparticle-coated target plates. The peptides used for external calibration were deposited on the plate to minimize the mass shift. The analyte surface was irradiated with 100 laser shots in the positive mode.

Results and discussion

Ability of the nanoparticles to assist ionization of pure sample analytes

We used the standard ginsenosides G-Rb_1 [exact mass (Me): 1108.6], G-Rb_2 (Me: 1078.6), G-Rc (Me: 1078.6), G-Rd (Me: 947.2), G-Re (Me: 947.2), G-Rf (Me: 800.5), and G-Rg_1 (Me: 800.5) to evaluate the usefulness of employing nanoparticles as laser

desorption/ionization materials. The mass spectra of the standard ginsenosides were obtained in the presence of nanoparticles with sodium ions, thereby ensuring that the precursor ions were obtained in the form of $[M + Na]^+$ ions (Taira et al. 2008). In this study, the standard ginsenosides formed sodium-adduct ions and yielded high-intensity signals. Further, to characterize a variety of ginsenosides, we performed post-source decay (PSD) MS for structural analysis.

For G-Rb_1, we obtained a precursor $[M + Na]^+$ ion at *m/z* 1132.1. This ion yielded fragment ions $[z1 + Na]^+$ (at *m/z* 789.3), which corresponded to the combination of the agricone moiety and disaccharide moiety of R_1 or R_2, and $[y1 + Na]^+$ (at *m/z* 364.7), which corresponded to the disaccharide moiety of R_1 or R_2 (Figure 2a).

Similarly, the PSD spectra of G-Rb_2 and Rc showed a precursor ion at *m/z* 1102.1 and the 2 derivative ions, namely, $[y1 + Na]^+$ at *m/z* 335.2, which corresponded to the disaccharide moiety of R_1, and $[z1 + Na]^+$ at *m/z* 789.8 (Figure 2b) and 789.6 (Figure 2c), which corresponded to the combination of the agricone and disaccharide moieties of R_2.

For G-Rd, we obtained an $[M + Na]^+$ ion at *m/z* 970.1 and 3 fragment ions at *m/z* 789.3, 365.2, and 203.1. The fragment ion $[z1 + Na]^+$ at *m/z* 789.3 corresponds to an R_1 molecule without the glucose moiety. The *m/z* values for the smaller fragment ions $[y2 + Na]^+$ and $[y1 + Na]^+$ (365.2 and 203.1, respectively) were consistent with the

molecular masses of sodium-adducted disaccharide and glucose moieties from R_2 and R_1, respectively (Figure 2d).

For G-Re (*m/z* of the precursor ion, 970.1), we obtained 2 fragment ions $[z1 + Na]^+$ and $[y1 + Na]^+$ at *m/z* values 789.2 and 203.1, respectively. The mass difference between the precursor ion and the fragment ion at *m/z* 789.2 was 180.9, which indicated the loss of a glucose molecule. The fragment ion at *m/z* 203.1 indicated a sodium-adducted glucose moiety from R_1 (Figure 2e). The same exact mass of R_f and Rg_1 showed difference in the PSD spectra. The PSD of G-Rf showed only 1 fragment ion $[z1 + Na]^+$ at *m/z* 365.2, which corresponded to the disaccharide moiety from R_3 (Figure 2f). In contrast, the PSD of G-Rg_1 showed 2 fragment ions, namely, $[z1 + Na]^+$ and $[y1 + Na]^+$ at *m/z* values 643.8 and 202.9, respectively, which corresponded to the agricone and glucose moieties of R_1 or R_3 and the divided glucose moiety from R_1 or R_3, respectively (Figure 2g). We distinguished the molecules with the same exact mass on the basis of the differences in the composition of disaccharides (G-Rf) and monosaccharides (G-Rg_1). These nano-PALDI PSD fragmentation patterns were in good agreement with the MALDI PSD fragmentation patterns of standard ginsenosides (data not shown). This finding indicated that our technique could also yield accurate results under mild ionization conditions without unnecessary degradation of the

bioactive molecule. These results could be utilized for analyzing the index of raw sample like plant extracts.

We observed a number of high-intensity signals for ginsenosides in the extract of *Panax ginseng* t mass spectra obtained with nanoparticles in the absence (Figure 3a) or presence (Figure 3b) of sodium ions. Although there were few MS signals with intensity greater than *m/z* 600, we could confirm the signals that corresponded to ginsenosides. In the case of the G-Rb_1 ions (*m/z* 1131.6 $[M + Na]^+$; 1147.6 $[M + K]^+$), both sodium- and potassium-adduct ions were observed in the absence of sodium acetate (Figure 3a inset), because the extract originally included salt ions, especially sodium and potassium salts. In the MS spectrum, such salt ions preferentially appeared in their adducted form, rather than the protonated form. However, the related signals showed a convergence only in the case of the sodium-adducted form (*m/z* 1131.2). Interestingly, the correlation between the signals of the sodium-adducted form of G-Rg_1 (*m/z* 823.1) and G-R_{b2} or R_c (*m/z* 1102.1) appeared only in the presence of sodium acetate (10 mM) (Figure 3b inset). In addition, the background noise in the presence of sodium acetate (Figure 3b inset), was lower than in the absence of sodium acetate (Figure 3a inset). The sodium-adducted forms of G-Rg_1 and G-Rb_2 or Rc were more easily ionized than other ion-adducted forms, such as the proton- or

potassium-adducted form. This result indicated that the ginsenosides had optimal ionization forms. Moreover, in the low molecular range (m/z 200–400), the signal intensities in the presence of sodium ions (Figure 3b), were lower than that in the absence of these ions (Figure 3a); thus, the signals in this region indicated a preferential ionization to the protonated form. This technique can be used for accurate and simple analysis of complex mixtures such as foods and nutrients; however, the differences in the ionization characters of these samples must be carefully considered while performing these analyses.

To perform structural analysis using post-source decay (PSD) nano-PALDI mass spectrometry, we deduced that the 4 signals at *m/z* 551.5, 823.1, 1102.4, and 1132.1 were obtained from the extract of *Panax ginseng* in the presence of sodium ion and determined that these signals originated from lysophosphatidylcholine (LPC)-(1-acyl 20:1) ($[M + H]^+$ ion), G-Rg_1 ($[M + Na]^+$ ion), G-Rb_2 or G-Rc ($[M + Na]^+$ ion), and G-Rb_1 ($[M + Na]^+$ ion). For the precursor $[M + H]^+$ ion of LPC-(1-acyl 20:1) at *m/z* 551.1, the typical fragment ions $[y1]^+$ and $[z1 + H]^+$ were detected at *m/z* 85.9 and 298.5, respectively; this finding provided information on the trimethylamine moiety and the fatty acid (1-acyl 20:1) in the sequence. The PSD fragment patterns indicated that the promptly obtained lipid fragment ions did not originate from the observed molecular

ions, because the prompt fragmentation occurred immediately after the formation of highly unstable protonated precursor ions (Figure 4a) (Al-Saad, Zabrouskov, Siems, Knowles, Hannan & Hill, 2003).

Similarly, the PSD spectra of ginsenosides showed fragment ions similar to those of the standard ginsenosides G-Rg_1, G-Rb_2 or G-Rc, and G-Rb_1. The PSD spectrum of G-Rg_1 showed 2 derivative ions that corresponded to the glucose ions (*m/z* 202.9; $[M + Na]^+$) of R_1 or R_2 and the agricone moieties (*m/z* 643.8; $[M + Na]^+$) (Figure 4b).

We detected a precursor ion at *m/z* 1102.1 and 2 derivative sodium-adduct ions at *m/z* 336.3 and *m/z* 789.0, which corresponded to the disaccharide moiety of R_1 or R_3 and the combination of the disaccharide and agricone moieties of R_1 or R_3, respectively. The difference between G-Rb_2 and G-Rc can be attributed to the arabinose conformation (arabinopyranose for G-Rb_2 and arabinofuranose for G-Rc) within the disaccharide moiety of R_2; this conformation can complicate the distinction between G-Rb_2 and G-Rc using the PSD MS technique (Figure 4c). The corresponding PSD spectrum of G-R_{b1} is shown in Figure 4d. We detected an $[M + Na]^+$ precursor ion at *m/z* 1132.1 and 2 fragment ions, namely, $[M + Na]^+$ at *m/z* 788.4 and $[M + Na]^+$ at *m/z* 365.0. These fragment ions could be considered as the z1 and y1 ions, which are characteristic of the cleavage of the glycosidic bonds at R_1 or R_2.

These fragment patterns were in good agreement with the PSD spectra of standard ginsenosides (Figure 2 a, b, c, and g). We could identify the bioactive components such as ginsenosides and lipids from the extract by using the nano-PALDI MS technique.

4. Conclusions

Nano-PALDI MS allowed ionization and background-free analysis of the small molecules in a *Panax ginseng* extract. The nanoparticles could ionize the standard ginsenosides in the presence of external sodium ions. The obtained signals corresponded to those of sodium-adduct ions. Although conventional matrices do not ionize the analyte in the presence of external salt ions, this technique can facilitate the analysis of crude samples like plant extracts. Using this technique, we detected lipids and ginsenosides in the *Panax ginseng* extract and identified the optimal ion forms of these compounds. We mainly focused on using nano-PALDI MS to investigate the role of ginsenosides as the active components of *Panax ginseng*. However, the contributions of other compounds, such as saccharides, peptides, and proteins, should be investigated. The nano-PALDI MS technique is a good substitute for MALDI and has great potential for rapid screening of bioactive ingredients such as ginsenosides in plant extracts; however, further studies are required to establish their traceability in foods and nutrient

product.

In addition, the nanoparticles may be utilized in the mass spectrometric analyses of biomedical tissues (Taira et al., 2008) and in cellular analysis (Moritake et al., 2009). The nanoparticle-based approach used in this study can be employed for simple and efficient identification of various ingredients of foods and herbal products used in TCM.

Acknowledgments

We thank member of Takagi and Takamura laboratory in JAIST, particularly Prof. M. Takagi and Prof. Y. Takamura, Ms. A. Makino and Ms T. Taniho for providing technical assistance and advice. This research was supported by a WAKATE-B grant from the Japan Society for the Promotion of Science to S. T. and a Grant-in-Aid to S. T. from JAIST and the resource of coordinated research program to Nitto Denko and a A-STEP to S. T. and Y. S. from Japan Science and Tech. Agency

Figure legends

Figure 1

A schematic illustration of nanoparticle-assisted laser desorption/ionization (nano-PALDI) mass spectrometry (a). Transmission electron microscopy (TEM) image of the nanoparticles (b). When reserpine (100 pmol) was used as a model drug with the nanoparticles, the nano-PALDI mass spectra (c) did not show any background

246 interference in the low-mass region. In contrast, the mass spectra of reserpine with
247 4-hydroxy-α-cinnamic acid (CHCA) showed background noise in the low-mass region
248 (d).

249

250 Figure 2

251 The post-source decay nanoparticle-assisted laser desorption/ionization (nano-PALDI)
252 mass spectra of the standard ginsenosides G-Rb_1 (a), G-Rb_2 (b), G-Rc (c), G-Rd (d),
253 G-Re (e), G-Rf (f), and G-Rg_1 (g). The abbreviations for the sugar moieties are glc
254 (β-D-glucose), arap (α-L-arabinose; pyranose), araf (α-L-arabinose; furanose), and rha
255 (α-L-rhamnose).

256

257 Figure 3

258 Mass spectra of the extract with nanoparticles (NPs) alone (a) and with NPs in the
259 presence of sodium acetate (NaAc: 10 mM) (b). The superimposed spectra of
260 tissue-cultured *Panax ginseng* (TCPG) extract with NPs in the absence (upper) and
261 presence of (lower) additional NaAc.

262

263 Figure 4

The post-source decay nanoparticle-assisted laser desorption/ionization (nano-PALDI) mass spectra of lysophosphatidylcholine (LPC)-(1-acyl 20:1) (a), ginsenoside (G)-Rg_1 (b), G-Rb_2 or G-Rc (c), and (G)-Rb_1 (d). The abbreviations for the sugar moieties are the same as those used in Figure 2.

References

Ai, K., Zhang, B., & Lu, L. (2009). Europium-based fluorescence nanoparticle sensor for rapid and ultrasensitive detection of an anthrax biomarker. *Angewandte Chemie. International Ed. In English*, *48*(2), 304-308.

Al-Saad, K. A., Zabrouskov, V., Siems, W. F., Knowles, N. R., Hannan, R. M., & Hill, H. H., Jr. (2003). Matrix-assisted laser desorption/ionization time-of-flight mass spectrometry of lipids: ionization and prompt fragmentation patterns. *Rapid Communications in Mass Spectrometry*, *17*(1), 87-96.

Chithrani, B. D., & Chan, W. C. (2007). Elucidating the mechanism of cellular uptake and removal of protein-coated gold nanoparticles of different sizes and shapes. *Nano Lett*, *7*(6), 1542-1550.

Cui, M., Song, F., Liu, Z., & Liu, S. (2001). Metal ion adducts in the structural analysis of ginsenosides by electrospray ionization with multi-stage mass spectrometry. *Rapid Communications in Mass Spectrometry*, *15*(8), 586-595.

Fuzzati, N., Gabetta, B., Jayakar, K., Pace, R., & Peterlongo, F. (1999). Liquid chromatography-electrospray mass spectrometric identification of ginsenosides in Panax ginseng roots. *Journal of Chromatography A*, *854*(1-2), 69-79.

Hijikata, Y., Miyamae, Y., Takatsu, H., & Sentoh, S. (2007). Two Kampo medicines, Jidabokuippo and Hachimijiogan alleviate sprains, bruises and arthritis. *Evidence-Based Complementary and Alternative Medicine*, *4*(4), 463-467.

Kalogianni, D. P., Koraki, T., Christopoulos, T. K., & Ioannou, P. C. (2006). Nanoparticle-based DNA biosensor for visual detection of genetically modified organisms. *Biosensors and Bioelectronics*, *21*(7), 1069-1076.

Kitada, S., Kikuchi, E., Ohono, A., Aramaki, S., & Maenosono, S. (2009). Effect of diamine treatment on the conversion efficiency of PbSe colloidal quantum dot solar cells *Solid State Communications*, *149*(41-42), 1853-1855.

Li, T. S. C., Mazza, G., Cottrell, A. C., & Gao, L. (1996). Ginsenosides in roots and leaves of American ginseng. *Journal of Agricultural and Food Chemistry*, *44*(3), 717-720.

Metori, K., Furutsu, M., & Takahashi, S. (1997). The preventive effect of ginseng with du-zhong leaf on protein metabolism in aging. *Biological and Pharmaceutical Bulletin*, *20*(3), 237-242.

Mitsudome, T., Noujima, A., Mizugaki, T., Jitsukawa, K., & Kaneda, K. (2009). Supported gold nanoparticle catalyst for the selective oxidation of silanes to silanols in water. *Chem Commun (Camb)*(35), 5302-5304.

Moritake, S., Taira, S., Ichiyanagi, Y., Morone, N., Song, S.-Y., Hatanaka, T., Yuasa, S., & Setou, M. (2007). Functionalized Nano-Magnetic Particles for an In Vivo Delivery System *Journal of Nanoscience and Nanotechnology*, *7*(3), 937-944.

Moritake, S., Taira, S., Sugiura, Y., Setou, M., & Ichiyanagi, Y. (2009). Magnetic nanoparticle-based mass spectrometry for the detection of biomolecules in cultured cells. *J Nanosci Nanotechnol*, *9*(1), 169-176.

Newman, M., Wu, J., Gardner, B., Munroe, K., Leombruno, D., Recchia, J., Kensil, C., & Coughlin, R. (1992). Saponin adjuvant induction of ovalbumin-specific CD8+ cytotoxic T lymphocyte responses. *Journal of Immunology*, *148*(8), 2357-2362.

Ravindranath, S. P., Mauer, L. J., Deb-Roy, C., & Irudayaraj, J. (2009). Biofunctionalized magnetic nanoparticle integrated mid-infrared pathogen sensor for food matrixes. *Analytical Chemistry*, *81*(8), 2840-2846.

Spelman, K., Burns, J., Nichols, D., Winters, N., Ottersberg, S., & Tenborg, M. (2006). Modulation of cytokine expression by traditional medicines: A review of herbal immunomodulators. *Alternative Medicine Review*, *11*(2), 128-150.

Sun, S., Wang, C. Z., Tong, R., Li, X. L., Fishbein, A., Wang, Q., He, T. C., Du, W., & Yuan, C. S. (2009). Effects of steaming the root of Panax notoginseng on chemical composition and anticancer activities. *Food Chemistry*, *118*(2), 307-314.

Taira, S., Hatanaka, T., Moritake, S., Kai, Y., Ichiyanagi, Y., & Setou, M. (2007). Cellular Recognition of Functionalized with Folic acid Nanoparticles. *e-Journal of Surface Science and Nanotechnology*, *5*, 23-28.

Taira, S., Kitajima, K., Katayanahi, H., Ichiishi, E., & Ichiyanagi, Y. (2009). Manganese oxide nanoparticle-assisted laser desorption/ionization mass spectrometry for medical applications. *Science and Techonology of Advanced Materials*.

Taira, S., Sugiura, Y., Moritake, S., Shimma, S., Ichiyanagi, Y., & Setou, M. (2008). Nanoparticle-assisted laser desorption/ionization based mass imaging with cellular resolution. *Analytical Chemistry*, *80*(12), 4761-4766.

Tawab, M. A., Bahr, U., Karas, M., Wurglics, M., & Schubert-Zsilavecz, M. (2003).

331 Degradation of ginsenosides in humans after oral administration. *Drug Metab□lism and*
332 *Disposition: The Biological Fate of Chemicals*, *31*(8), 1065-1071.
333 Wang, Y. T., You, J. Y., Yu, Y., Qu, C. F., Zhang, H. R., Ding, L., Zhang, H. Q., & Li, X. W.
334 (2008). Analysis of ginsenosides in Panax ginseng in high pressure microwave-assisted
335 extraction. *Food Chemistry*, *110*(1), 161-167.
336 Wu, J., Gardner, B., Murphy, C., Seals, J., Kensil, C., Recchia, J., Beltz, G., Newman, G., &
337 Newman, M. (1992). Saponin adjuvant enhancement of antigen-specific immune responses
338 to an experimental HIV-1 vaccine. *Journal of Immunology*, *148*(5), 1519-1525.
339 Xu, H., & Xu, H. E. (2009). Analysis of trace elements in Chinese therapeutic foods and
340 herbs. *American Journal of Chinese Medicine*, *37*(4), 625-638.
341 Yang, M., Kostov, Y., Bruck, H. A., & Rasooly, A. (2009). Gold nanoparticle-based enhanced
342 chemiluminescence immunosensor for detection of Staphylococcal Enterotoxin B (SEB) in
343 food. *International Journal of Food Microbiology*, *133*(3), 265-271.
344 Zeng, Z. D., Liang, Y. Z., Jiang, Z. H., Chau, F. T., & Wang, J. R. (2008). Quantification of
345 target components in complex mixtures using alternative moving window factor analysis
346 and two-step iterative constraint method. *Talanta*, *74*(5), 1568-1578.
347
348

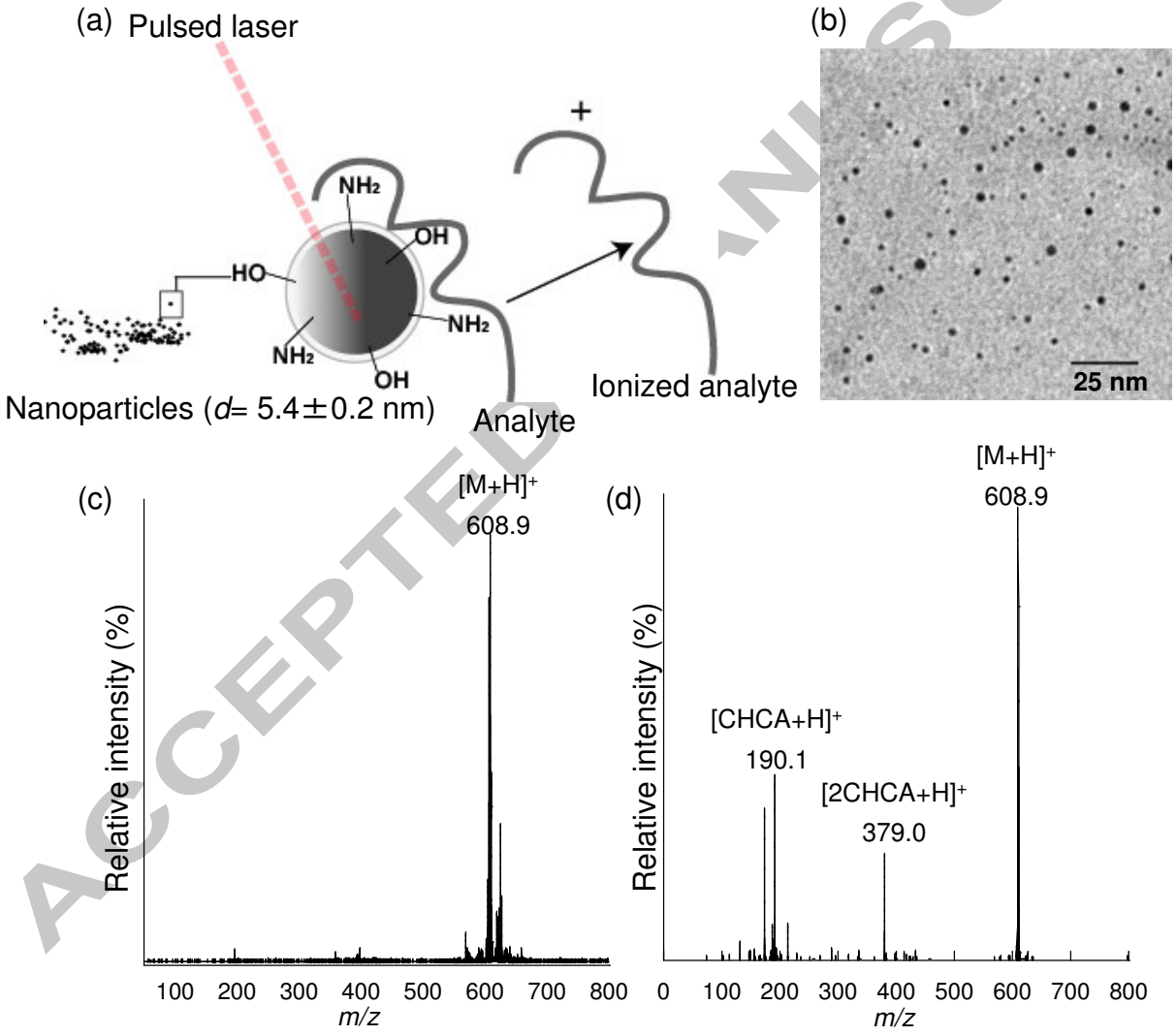

Figure 1 Taira et al.

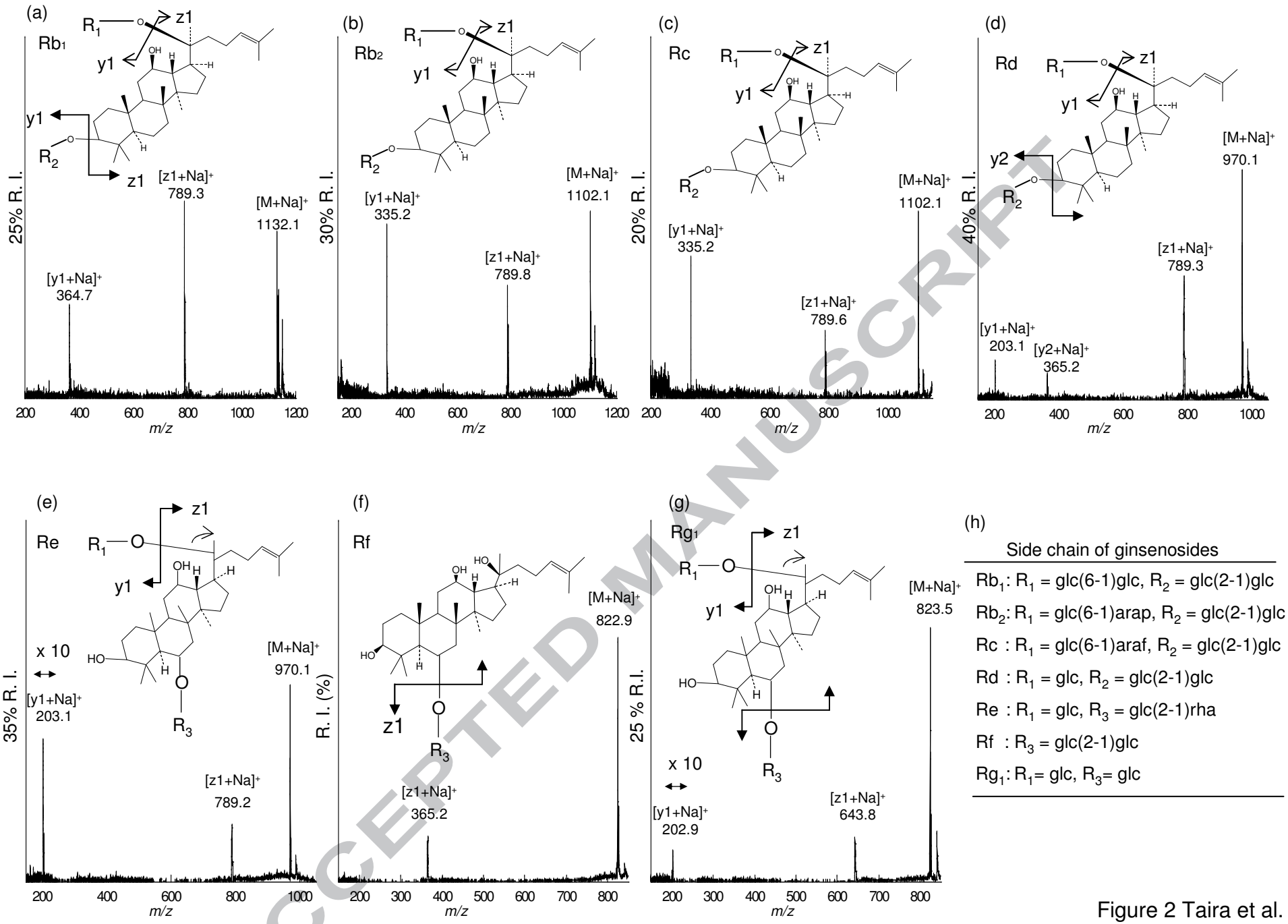

Figure 2 Taira et al.

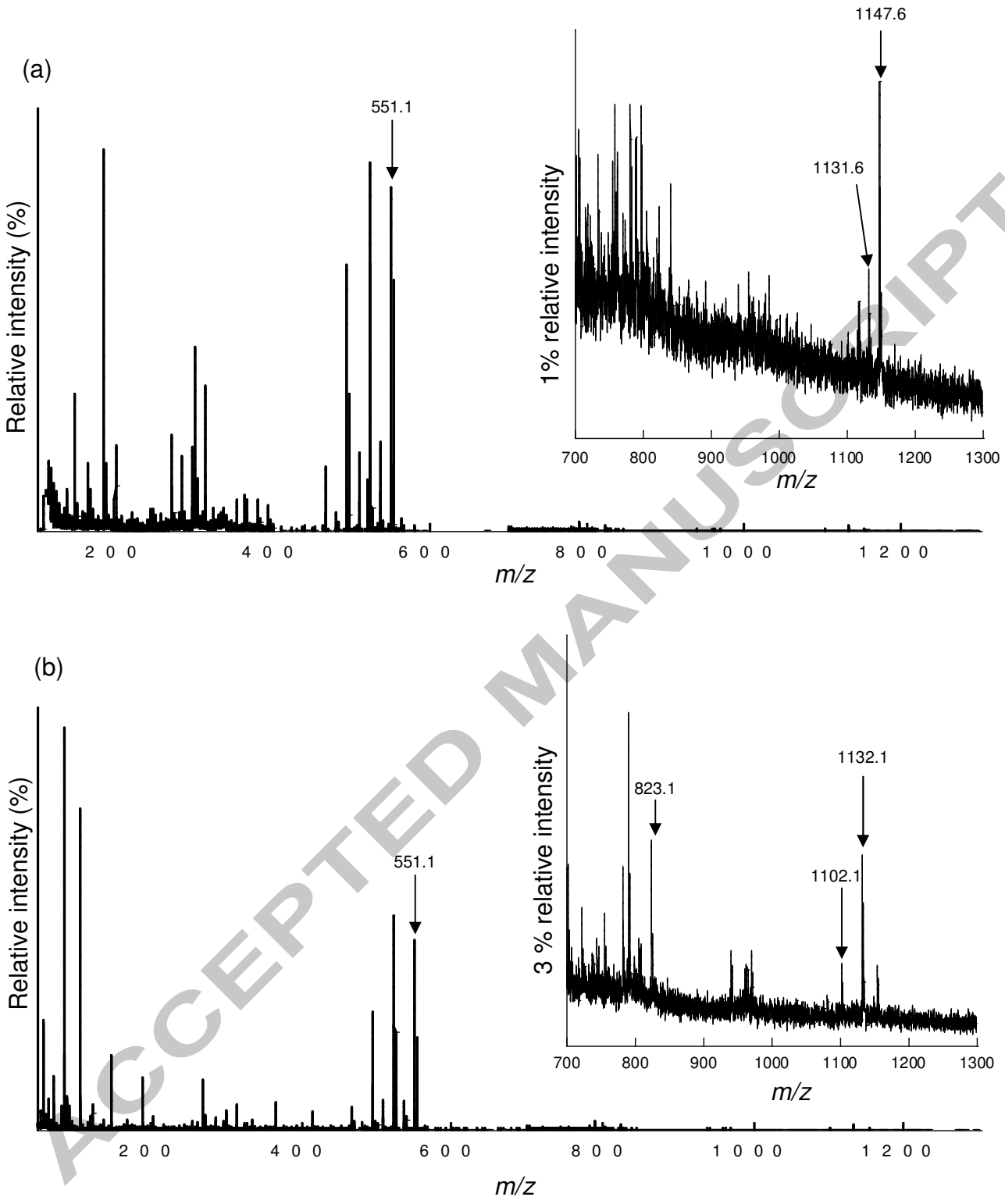

Figure 3 Taira et al.

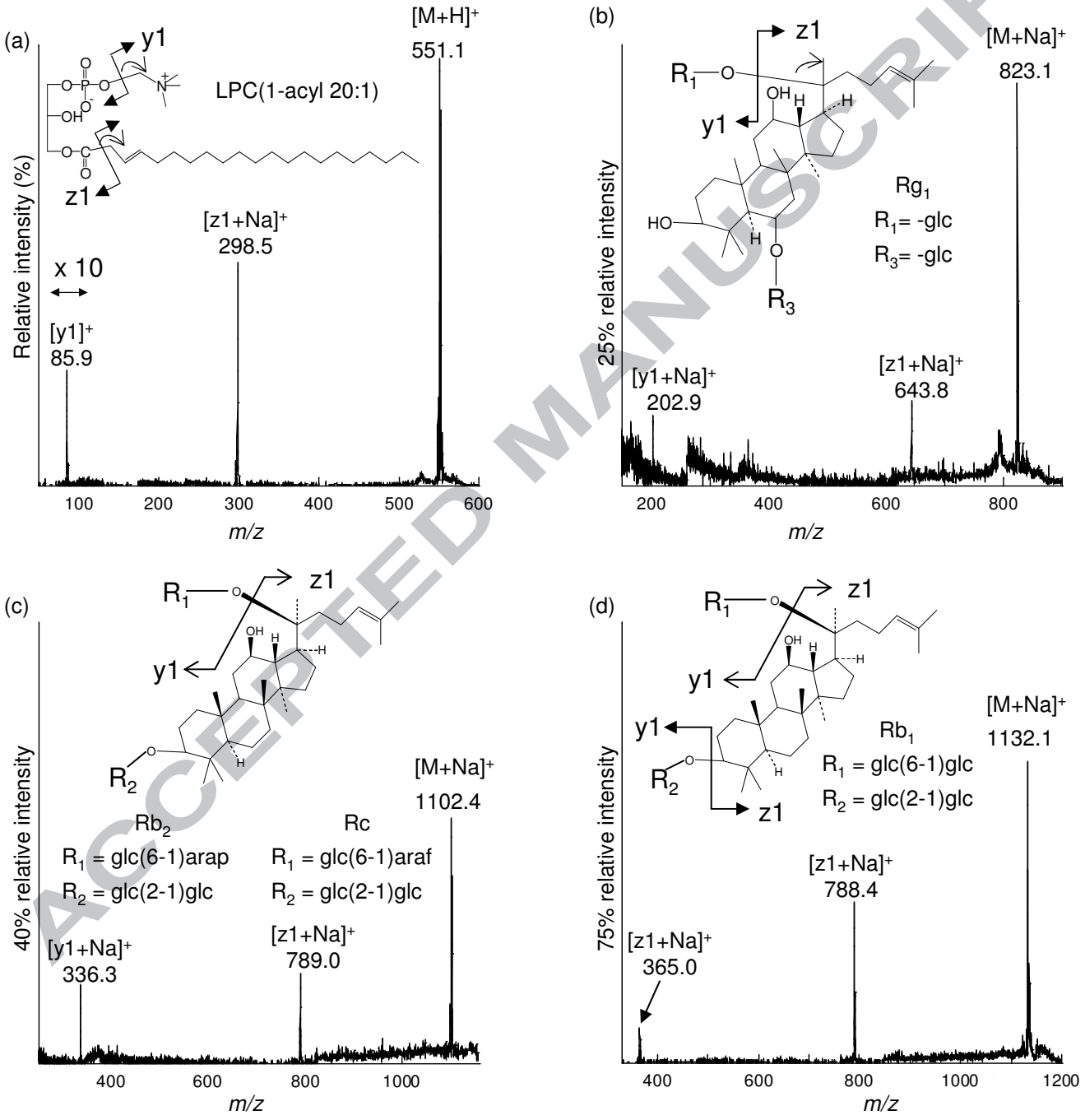

Figure 4 Taira et al.